IEEE Journal of Microwaves

Received 1 July 2024; revised 20 August 2024; accepted 22 August 2024. Date of publication 18 September 2024; date of current version 2 December 2024.

*Digital Object Identifier 10.1109/JMW.2024.3450015*

# Towards Detecting Climate Change Effects With UAV-Borne Imaging Radars

**INGRID ULLMANN [1] (Member, IEEE), CHRISTINA BONFERT [2] (Member, IEEE), ALEXANDER GRATHWOHL [2] (Graduate Student Member, IEEE), MOHAMED AMINE LAHMERI [1] (Member, IEEE), VICTOR MUSTIELES-PÉREZ [1,3], JULIAN KANZ [2] (Graduate Student Member, IEEE), ELENA STERK [2], FREDERIK BORMUTH [2] (Graduate Student Member, IEEE), ROGHAYEH GHASEMI [1] (Graduate Student Member, IEEE), PATRICK FENSKE [1] (Member, IEEE), MICHELANGELO VILLANO [3] (Senior Member, IEEE), ROBERT SCHOBER [1] (Fellow, IEEE), ROBERT F. H. FISCHER [2] (Senior Member, IEEE), GERHARD KRIEGER [1,3] (Fellow, IEEE), CHRISTIAN DAMM [2] (Member, IEEE), CHRISTIAN WALDSCHMIDT [2] (Fellow, IEEE), AND MARTIN VOSSIEK [1] (Fellow, IEEE)**

*(Invited Paper)*

[1]Friedrich-Alexander-Universität Erlangen-Nürnberg, 91058 Erlangen, Germany
[2]Ulm University, 89081 Ulm, Germany
[3]Microwaves and Radar Institute, German Aerospace Center (DLR), 82234 Wessling, Germany

CORRESPONDING AUTHOR: Ingrid Ullmann (e-mail: ingrid.ullmann@fau.de).

This work was supported by Deutsche Forschungsgemeinschaft (DFG, German Research Foundation) under GRK 2680 – Project-ID 437847244.

**ABSTRACT** Climate change is associated with a variety of environmental phenomena, such as the melting of glaciers, the drying out of crops and soils, and an increase in the risk of avalanches. To detect and monitor these changes, satellite-based radar imaging is widely used, as it enables the large-scale mapping of the Earth's surface independent of weather and sunlight. An emerging field of research is to use radar systems mounted on unmanned aerial vehicles (UAVs) for this purpose. UAV-borne radar systems image smaller areas, but can capture them in greater detail, more flexibly in terms of flight trajectory, and at shorter repetition intervals. This article presents the capabilities of UAV-based radar systems and the associated challenges in terms of system design and imaging techniques for detecting and monitoring the effects of climate change. Current research results are shown. In addition, we give an outlook on using a swarm of cooperative UAVs, each carrying a radar. UAV swarms will enable a higher imaging quality with respect to resolution and detectability, but at the same time come with a number of additional challenges, which will be discussed in the paper as well.

**INDEX TERMS** Climate change, microwaves in climate change, radar, radar imaging, remote sensing, UAV.

## I. INTRODUCTION

Climate change will have far-reaching consequences for the environment. Prominent examples are the melting of glaciers, the desertification of soils, permafrost thawing, and the increased risk of landslides and avalanches. A systematic monitoring of these changes and risks will help to improve our scientific understanding of the impacts of climate change on our natural and man-made environment and will help decision-makers to mitigate the associated consequences.

Radar is a remote sensing technology that can contribute to this complex task. It works independently of light and weather conditions, thus, it is operable even at night or in foggy weather. Airborne and spaceborne radar systems operating according to the synthetic aperture radar (SAR) principle have been used to monitor geophysical properties for a long time [1], [2], [3]. They have provided knowledge about the Earth's topography [4], the structure of glaciers [5], [6], [7], flooding [8], soil moisture [9], [10], and vegetation development [11],

© 2024 The Authors. This work is licensed under a Creative Commons Attribution-NonCommercial-NoDerivatives 4.0 License. For more information, see https://creativecommons.org/licenses/by-nc-nd/4.0/

**FIGURE 1. Photograph of our UAV-borne radar system flying over the aletsch glacier in Switzerland. High-resolution radar images, digital elevation models and tomograms of the earth can potentially be produced with such systems. The radar system on the photo was introduced in [13].**

[12], all of which can be indicators of climate change. While airborne and spaceborne radar imaging are well-established techniques for large-scale monitoring, they come with some disadvantages when smaller areas are of interest. Satellites take days or weeks to observe again the same point on Earth, which may be too long to unambiguously monitor fast-changing effects or sudden phenomena. Furthermore, the missions are costly and require extensive planning. This restricted temporal resolution of spaceborne SAR systems is further accompanied by a limited spatial resolution, which often prevents the observation and analysis of small-scale processes on the Earth's surface.

Therefore, for imaging local geographic developments, an interesting alternative is the use of unmanned aerial vehicles (UAVs) that carry a radar system. For illustration, Fig. 1 shows a UAV equipped with a radar system flying over the Aletsch Glacier in Switzerland.

While UAV-borne radar imaging systems cannot monitor the whole Earth, they can be useful on a local scale. The main advantages of UAV-based systems are their reduced operating costs, their easy deployment and their flexibility in terms of flight trajectory [14], [15]. Additionally, it is possible to use higher operating frequencies compared to air- or spaceborne systems since the distances between sensor and target area are much smaller. Using higher frequencies will enable higher image resolutions and thus a more detailed information compared to spaceborne SAR.

Therefore, UAV-borne radar imaging is a promising technique for local remote sensing and monitoring. It also provides opportunities to demonstrate innovative techniques before implementing them in space. To operate UAV-borne radar imaging systems several requirements have to be considered. This article discusses potentials and challenges of UAV-borne SAR systems in the context of environmental monitoring. We review the related state of the art, address various aspects ranging from system design to imaging techniques, and present recent results from our research group. In particular, system design covers the aspects of the radar system itself, its embedding on the UAV, the choice of an optimal flight path, and the fulfilment of UAV localization requirements.

Various radar imaging techniques can be used to evaluate the data acquired by a UAV-borne radar. Interferometric and tomographic approaches are classically used in Earth remote sensing and can be adapted. Since the UAV flight paths might be non-uniform due to, e.g., wind and instability, the data are potentially subsampled or non-uniformly sampled. For processing subsampled data, compressed sensing methods can be applied. When subsurface structures are of interest, such as soil layers, dedicated subsurface imaging algorithms must be used. All these aspects will be detailed in the paper.

As a future prospect, we discuss using UAV swarms operating simultaneously. This concept has only been developed to a limited extent to date, but holds great potential. Using a cooperative and possibly coherent radar network distributed across several UAVs will enable faster measurements of larger areas, higher resolution, and better scalability. Capturing bi- and multistatic SAR images will become possible this way, as well as single-pass interferometry and tomography.

At the same time, additional challenges arise for both system design and imaging. In particular, this includes the synchronization of the individual radars. Coherence is an additional challenge since the individual radars are not physically connected. However, a coherent radar network would be very attractive, e.g., for bistatic SAR.

From the above discussion, it becomes clear that monitoring climate change with UAV-borne radar is a manifold engineering task. The focus of this paper is to cover this field as a whole, detailing the aspects of system design (Section II), imaging (Section III), and the idea of cooperative UAV swarms (Section IV). We discuss the associated challenges and currently investigated solutions. Conclusions and an outlook will be given in Section V.

## II. SYSTEM DESIGN FOR UAV-BORNE RADARS

UAV-borne radar systems are currently being developed for a wide range of surface and subsurface imaging applications. An overview of existing systems will be given in Section II-A. In designing such systems, care must be taken regarding localization accuracy, which will be detailed in Section II-B. One benefit of UAV-based radar is that flight paths can be selected arbitrarily. The flight trajectory is therefore another design parameter in UAV-based radar imaging. For this, optimization strategies will be discussed in Section II-C.

### A. EXISTING SYSTEMS

The scattering properties of soils, ice, plants, and structures differ significantly between frequency bands. Therefore, depending on the application, UAV-based SAR systems have been developed for a wide range of frequencies from UHF-band [16], to L-band [17], S/C-band [18], [19], X-band [20], [21], [22], and K-band [23]. These radar systems use classical

remote sensing techniques to create SAR images. Additionally, some attempts have been made to extract additional information using tomography [16] and interferometric SAR methods [17], [21].

Systems for ground penetrating imaging mostly operate at L/S-band or at lower frequencies to limit losses in the ground. The radar systems differ significantly depending on the targeted application. While some target the detection of buried objects or structures [24], [25], [26], [27], [28], [29], others focus on the investigation of layers in snow and ice [30], [31], [32], [33] or properties of the soil itself [34].

### B. LOCALIZATION REQUIREMENTS

Surface and subsurface imaging can be achieved using a wide range of methods; which will be detailed in Section III. All methods require that the positions of the radar antennas are known along the measurement trajectory. The required localization accuracy depends on the imaging resolution, and therefore the evaluation method employed for imaging. Methods range from simple low-resolution scanning techniques to high-resolution SAR processing (see Section III). If simple scanning techniques are used, the required localization accuracy is only limited by the allowed geometric distortions in the resulting image. Ideally, the accuracy should be better than the range resolution of the radar, which depends on its bandwidth. For existing down-looking systems the required accuracy is 2.5 cm – 10 cm, derived from a bandwidth of 1.5 GHz – 6 GHz.

High-resolution imaging using SAR imposes higher demands. The localization must be accurate enough to maintain phase coherency between radar measurements. The required accuracy is dependent on the radar center frequency [35]. For UHF-band systems, this already leads to accuracy requirements in the single-digit centimeter range, for L-band systems the required accuracy is around 1 cm [36]. For higher frequencies, especially X-band and above, the requirements can be relaxed by employing autofocus algorithms [21], [22], [23].

To measure the three-dimensional (3D) platform's position, satisfying the required accuracy, most systems rely on global navigation satellite systems (GNSS). With simple scanning, some down-looking systems exclusively use GNSS information [30], [34]. For high-resolution SAR imaging, this is not sufficient. Therefore, most such systems exploit measurements from an additional sensor to improve localization accuracy. Although using the radar itself for improved accuracy has been investigated [37], [38], [39], most systems rely on an inertial measurement unit (IMU) as their additional sensor [20], [21], [22], [23], [40]. This is because radar antennas are usually not mounted in the system's center of mass. Therefore, a high localization accuracy requires a precise UAV position as well as accurate attitude information.

Another source of positional errors is the GNSS itself. Real-time kinematic (RTK) or post-processed kinematic (PPK) GNSS [17], [19], [25], [31], [32] can provide a more accurate position using a base station. The station includes a GNSS receiver that is known to be static and can be used to cancel out drifts over time. Some systems even combine both precise RTK/PPK GNSS position and IMU data [17], [18], [26], [27], [28], [29], [33] to achieve highly accurate position and attitude information.

The system presented in Fig. 1 allows for an evaluation using SAR, yielding high-resolution images. As discussed above, this poses high requirements on the accuracy of localization. Therefore, we also rely on RTK GNSS measurements fused with IMU data. The applied method is presented in detail in [41].

### C. RESOURCE ALLOCATION AND FLIGHT TRAJECTORY OPTIMIZATION

UAVs suffer from limited resources compared to air- and space-borne systems. Overcoming this challenge requires careful optimization of the UAV trajectory and available resources to maximize performance. In this context, the authors in [42] studied the trajectory optimization for multistatic UAV-based SAR sensing in harsh environments, where the formulated constrained multi-objective optimization problem (CMOP) was solved based on heuristics. In [43], the authors studied resource allocation and trajectory optimization for multi-UAV SAR sensing where observation angle diversity, resolution, and image quality were considered. In [44], path planning optimization for a passive geosynchronous bistatic SAR system was formulated as CMOP and solved based on evolutionary algorithms. Furthermore, the authors in [45] investigated trajectory optimization for UAV-SAR to minimize power consumption while meeting constraints on spatial resolution and coverage. Taking into account real-time SAR, [46] presented a 3D trajectory and resource allocation optimization framework for maximizing SAR coverage while satisfying sensing and real-time communication constraints. While the previously mentioned works did not account for UAV instabilities affecting the sensing performance, [47] proposed a robust trajectory and resource allocation design to maximize the SAR coverage while meeting communication and sensing performance constraints. Although high-resolution two-dimensional (2D) SAR images are essential for environmental monitoring, 3D SAR imaging provides more sophisticated features that help in visualizing and analyzing the impact of climate change on Earth, e.g., reporting accurate changes in topography and small surface displacements in time. Few optimization frameworks were proposed in this context. [48] investigated formation and resource allocation for communication-assisted across-track interferometry using two UAVs. In this work, the two 3D trajectories and resources are jointly optimized to maximize the interferometric coverage while satisfying energy, communication, and sensing constraints.

## III. IMAGING TECHNIQUES

Following the system design, imaging algorithms are the core of radar-based environmental monitoring. A number of techniques exist for spaceborne SAR imaging and can be adapted

to the UAV case. Typical imaging techniques which can be used to monitor climate-induced effects will be presented in the following: Starting from a general description of SAR imaging algorithms (Section III-A), SAR interferometry will be described and illustrated by a recent measurement example (Section III-B). With interferometry, digital elevation models (DEMs) can be computed, which provide information on, e.g., glacier heights. To allow for 3D imaging, SAR tomography is employed, which will be detailed in Section III-C. Section III-D deals with Compressed Sensing, which is a popular technique for processing data, which is subsampled with respect to the spatial sampling theorem. This is particularly interesting for UAVs because, subsampling can occur due to flight path inaccuracies. Finally, in Section III-E, we discuss techniques for subsurface imaging, which differ from surface imaging due to the material interfaces involved.

### A. SAR IMAGING ALGORITHMS

SAR images can be reconstructed from the measurement data by using the Backprojection algorithm (BPA, cf. [36]), the Omega-k algorithm [49] and more. Backprojection numerically inverts the electromagnetic wave propagation by means of a spatial matched filter, which is the complex conjugate of the Green's function. Whereas Backprojection operates in the time-space domain, the Omega-k algorithm operates in the frequency-wavenumber domain. The Omega-k algorithm is much faster than the Backprojection algorithm; however, Backprojection also allows to directly process arbitrary and non-linear flight tracks as they are typically provided by UAVs.

### B. INTERFEROMETRY

Synthetic aperture radar interferometry (InSAR) is a powerful and well-established remote sensing technique that exploits the phase difference between two coherent SAR images to measure range differences with accuracies of a fraction of the wavelength [50]. InSAR enables very accurate measurements of a range of bio- and geophysical parameters that are of paramount importance for understanding the natural dynamics on the Earth's surface in times of accelerated climate change [3], [51].

InSAR is also well-known for providing accurate digital elevation models, which can be used to monitor terrain topography and soil properties, among others [52]. Furthermore, a time series of multiple DEMs provides information of elevation changes, e.g., due to subsidence, earthquakes, or ice movements in glaciers. Due to their versatility and ease of use, UAVs will enable frequent and systematic measurements of such changes on a local scale.

The quality of the DEMs is usually specified in terms of horizontal resolution or posting and height accuracy. The wide bandwidth that can be employed in UAV-borne radars along with the use of multiple baselines, e.g., provided by a swarm of several UAVs, allows for the generation of DEMs with height accuracies in the order of a decimeter (standard deviation) at a posting smaller than 20 cm $\times$ 20 cm [53].

**FIGURE 2. Optical image of the DEM in Fig. 3.**

This performance implies a resolution improvement of almost two orders of magnitude, when compared to DEMs obtained with state-of-the-art air- and spaceborne InSAR systems that can achieve DEM height accuracies and resolutions in the order of a meter [54], [55]. To demonstrate this performance improvement, we performed a measurement campaign using an ultra-wideband UAV SAR mounted on a multicopter [56]. Interferometric baselines ranging from 0.5 m to 2 m were generated by means of repeat-pass interferometric acquisitions, with an average UAV flying height of 30 m above ground level. The frequency-modulated continuous-wave (FMCW) radar system onboard the UAV acquired data with a bandwidth of 3 GHz in two different frequency bands with center frequencies of 2.5 GHz and 7.5 GHz, respectively. The interferometric SAR data were focused using a fast Omega-k algorithm and further processed to generate DEMs making use of the different baselines and the two frequency bands, yielding DEMs with an average height accuracy (standard deviation) of 12 cm at a horizontal resolution of 15 cm $\times$ 15 cm [56]. To illustrate the extraordinary quality of the DEMs obtained with such a system, we consider here a small patch of the imaged area that contains a transition from grass to bare ground, as shown in the optical image of Fig. 2, representing a very subtle topographic change of a few centimeters.

Fig. 3(a) depicts the topographic profile acquired with a 3D laser scanner, Fig. 3(b) shows the DEM obtained by means of multiple interferometric baselines in the frequency band of 6 GHz – 9 GHz, and Fig. 3(c) shows a histogram of the height errors between the two. The achieved standard deviation of the height errors is 7 cm at a posting of 20 cm $\times$ 20 cm.

In view of the large fractional bandwidth of UAV-borne radars, the frequency dependence of the InSAR coherence, i.e., the normalized complex cross-correlation between a pair of SAR images, can be further exploited to monitor changes in the physical properties of semi-transparent volumes, such as vegetation or soil, with a single baseline.

This technique was successfully used to estimate the volume height and frequency-dependent attenuation from simulated data [57]. Initial analyses to assess the penetration of the signal in the ground using interferometric data from the experiment described above have also been performed [58]. Future investigations will include the evaluation of soil moisture changes, which are a key parameter for understanding climate change, by using the information on penetration depth.

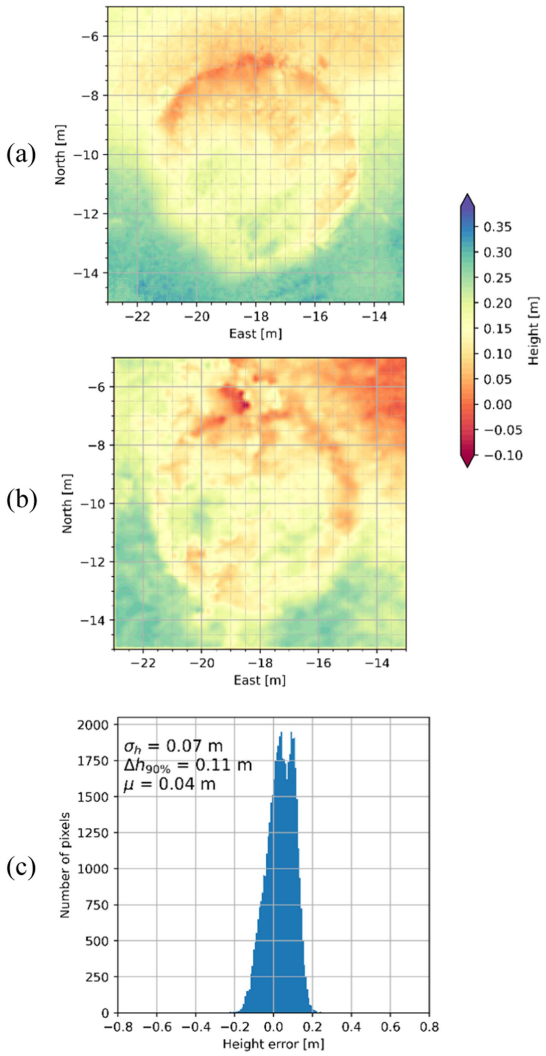


**FIGURE 3.** DEMs of the area shown in Fig. 2: (a) ground truth obtained with the laser scanner, (b) multi-baseline InSAR DEM in the frequency band 6 GHz – 9 GHz, and (c) histogram of errors.

### C. SAR TOMOGRAPHY

Although SAR interferometry, as discussed in the previous section, is able to estimate the ground height and thus ground topography by comparing the phases of two SAR images obtained at two different flight paths, it does not allow determining the height or elevation of different objects within a single pixel or to distinguish them in elevation. However, to monitor and image environmental structures, ecosystems or vegetation that are composed of different layers, such as forests, cropland, soil, ice or snow, 3D imaging is crucial to avoid layover and to investigate different structural properties. In contrast to interferometry, SAR tomography goes a step further and enables actual 3D imaging by capturing the environment along a large number of vertically spaced (parallel) trajectories to cover a variety of viewing angles. Airborne SAR tomography has been shown to be useful in climate and environmental monitoring, e.g., for mapping and investigating forest structures [59], estimating biomass [60], and mapping different ice layers [7]. To this end, compared to fixed-wing airborne or space-based systems, UAV-based SAR systems can easily realize multi-baseline and repeat-pass measurements at almost any height and for arbitrary track configurations.

Similar to the azimuth dimension, the resolution and unambiguous range in elevation depend on the covered aperture and sampling rate in height realized through the different baselines. Assuming perfect equidistant tracks of vertical spacing $d$, the maximum unambiguously resolvable volume height is proportional to $r_0/d$ [61], with $r_0$ the minimum range between track and scene. Compared to space-based systems, $r_0$ is much smaller for UAV systems. Therefore, with decreasing distance to the scene, smaller baselines of some meters or even less are sufficient. On the other hand, due to the lower flight altitudes, a wider range of elevation angles can be easily realized with UAVs, yielding a high height resolution [61]. However, it must be considered that if the aperture is to be increased, also the number of tracks must be increased. Thus, the trade-off between vertical resolution and unambiguous height is important in UAV-based SAR tomography.

To obtain 3D SAR images from measurements, different techniques are applied. Single-pass circular trajectories orbiting an area of interest allow unambiguous 3D imaging by applying, e.g., the Backprojection algorithm. Circular trajectories have been shown to be suitable for UAV-based ground-penetration applications where the height information of a limited area is investigated [62]. Circular tracks are easily realized with UAVs. However, circular trajectories are not suitable to cover large areas, as required in many environmental monitoring applications. Better suited for such applications are multi-pass parallel tracks at different heights covering a desired vertical baseline. 3D SAR imaging in this case is often realized by first processing 2D images of each track and afterwards performing an additional focusing in the elevation direction by combining the image data from the multiple tracks. Here, often sparsity-based methods are used [63]. A drawback of this approach is that, due to range migration, co-registration of the 2D images of the individual tracks is required to align the 2D grids. Finally, the Backprojection algorithm allows a direct generation of 3D images without the need of alignment and co-registration of the data as long as the measurements of the different tracks are temporarily correlated.

Fig. 4 shows a comparison of two UAV-based measurements of a single target (reflector) on ground. The average UAV flight height and ground range to the target was about 20 m and 15 m, respectively. In total 23 vertically spaced baselines are acquired with a total aperture of about 21 m. If only a single baseline is evaluated using the 3D backprojection (see Fig. 4, top row), the target is ambiguous in the ground-range-height-plane and the true target height above ground cannot be determined. However, if multiple baselines are evaluated (see Fig. 4, bottom row), the target can be unambiguously located in all three dimensions.

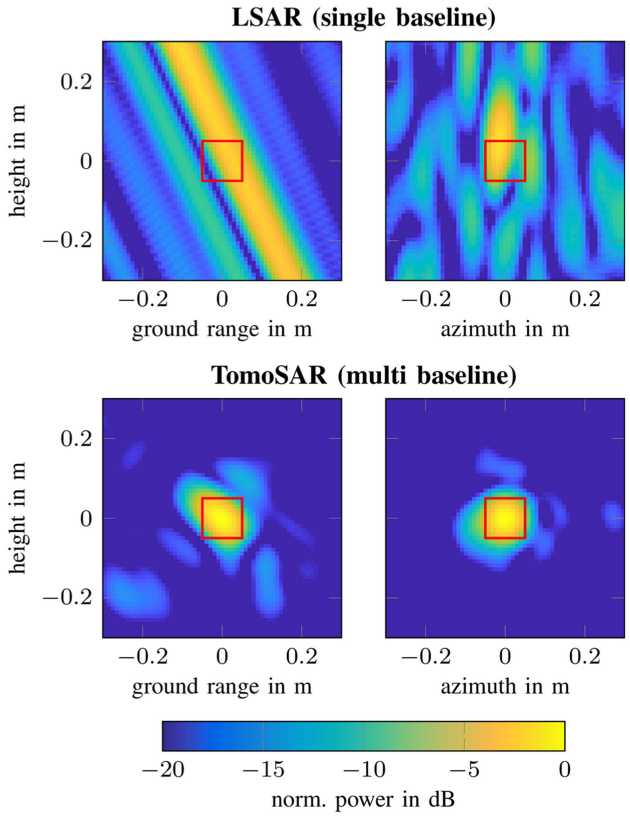


**FIGURE 4.** 3D SAR imaging results for a single target (reflector) using an LSAR single baseline measurement (top row) and a TomoSAR multi-baseline measurement (bottom row) acquired by a UAV-based radar. The multi-baseline setup consisted of 23 vertically spaced linear baselines with a total aperture of 21 m at an average height above ground of 20 m and an average ground range distance of 15 m. The true target position is marked by the red box. The images are obtained using the 3D-Backprojection approach.

### D. COMPRESSED SENSING

UAV-based radar imaging is limited by the Rayleigh resolution prescribed by the data acquisition rate and the effective aperture. Especially for UAV-based SAR monitoring of the natural environment, dense measurements and a huge amount of data must be collected and processed. Compressed sensing (CS) theory states that it is possible to reconstruct signals from (much) fewer measurements than required by the Shannon-Nyquist theorem under the condition that the signal itself is sparse or that it can be sparsely represented in some basis [64]. This can be written as:

$$\boldsymbol{y} = \boldsymbol{A}\boldsymbol{\Phi}\boldsymbol{x} + \boldsymbol{n} \tag{1}$$

with the observation $\boldsymbol{y} \in \mathbb{C}^{\mathrm{M}}$, the measurement matrix $\boldsymbol{A} \in \mathbb{C}^{\mathrm{M} \times \mathrm{N}}$, $M < N$, the basis $\boldsymbol{\Phi} \in \mathbb{C}^{\mathrm{N} \times \mathrm{N}}$, the sparse vector of coefficients $\boldsymbol{x} \in \mathbb{C}^{\mathrm{N}}$, and the measurement noise $\boldsymbol{n} \in \mathbb{C}^{\mathrm{M}}$. Given the observation $\boldsymbol{y}$, the task of a reconstruction algorithm is to produce an estimate of $\boldsymbol{x}$ and thus of the desired signal $\boldsymbol{\Phi}\boldsymbol{x}$.

Hence, CS has the potential to improve UAV-based SAR imaging while reducing the sampling and data acquisition effort, especially across large areas. A commonly used sparse representation in radar imaging and SAR in particular is the radar image itself where, compared to the image pixel number, only a few pixels contain strong scatterers. However, the signal may also be sparsely represented in other domains.

In the last few years, CS has been successfully introduced in the context of SAR [65], [66], [67] and also UAV-based SAR [68], [69], [70]. As CS has been shown to be especially suitable in the context of SAR tomography [63], [71], it offers great potential to facilitate UAV-based SAR monitoring of different vegetation layers, e.g., in forests, or soil and ice layers. However, due to the high resolution, large amount of data, and number of pixels in SAR images, as well as the low flight altitude of UAVs across man-made and natural environments, diverse challenges arise when CS is to be applied. Firstly, often the complexity and size of the CS problem become quite large in SAR imaging, as they are proportional to the number of pixels and samples that must be processed. It is therefore crucial to define a suitable basis which allows efficient transformation and a sparse representation. In addition, low-complexity algorithms such as the approximate message passing (AMP) algorithm [72] are often sufficient, especially when damping is used [73], however better-performing but computationally more demanding algorithms (e.g., [74]) are also of interest.

Beyond that, a major challenge is that the scene is not (sufficiently) sparse. Due to the relatively small distance between the UAV and scene and the high resolution that can be achieved in UAV-based SAR, objects are often spread across multiple pixels [70]. As a consequence, these pixels and thus sparse coefficients are correlated and contain unknown structural properties, which violates CS requirements, i.e., of point-like and uncorrelated sparse coefficients. Another major issue is the occurrence of clutter, which is very common in low-altitude SAR in natural environments and ground penetration. Clutter is undesirable but behaves like actual targets. It therefore interferes with the recovery of correct targets and makes robust CS recovery challenging.

An ongoing challenge is the extent of prior knowledge utilized in the algorithms, i.e., the degree of adaptation of the reconstruction algorithms to the scene. This is a trade-off between increasing the algorithms' complexity when including more prior knowledge, and the risk of decreased robustness to variations and model mismatches.

Fig. 5 shows an example for the application of CS with an improved Backprojection-based sensing matrix for UAV-based SAR imaging [70]. For recovery, a complex approximate message passing (CAMP) algorithm [75], [76] with adapted threshold that takes clutter into account is applied to a vastly reduced set of collected data. An improved clutter suppression, image quality, and sidelobe level is achieved even in case of severe clutter perturbation (gravel terrain) or bad focusing of the target (grass terrain).

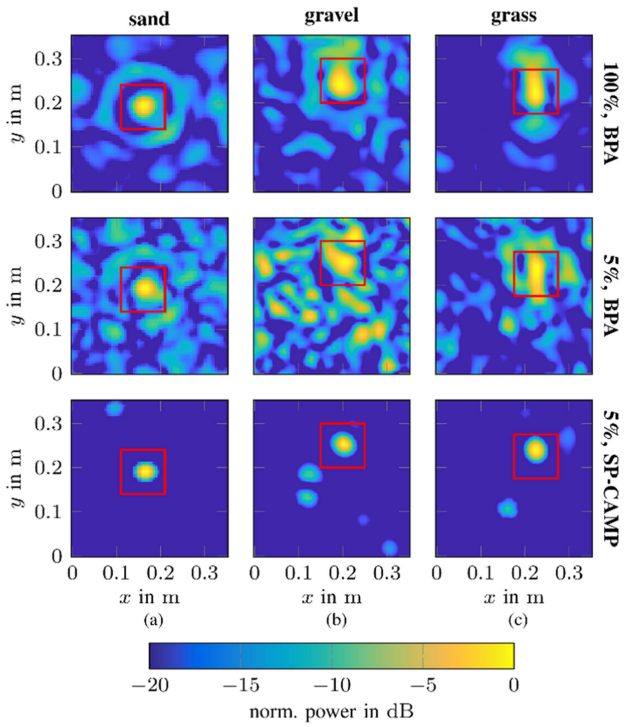


**FIGURE 5.** Measurement of a can lid buried in (a) sand, (b) gravel, and (c) grass. The measurements are evaluated (top to bottom) via the backprojection algorithm using 100% and 5% of the entire data, and via the adapted BPA-based CAMP using 5% of the data. The red boxes mark the ground truth positions of the targets. Figure taken from [70].

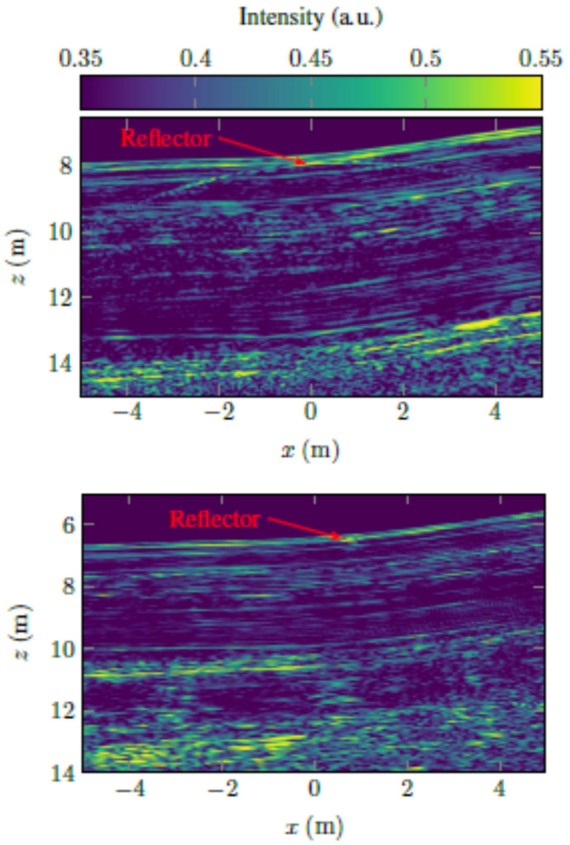


**FIGURE 6.** Example B-scan (top) and SAR image (bottom) acquired with a UAV-borne radar at the jungfraufirn glacier in Switzerland (taken from [82]). A corner reflector was buried in the ground as a reference target.

### *E. SUBSURFACE IMAGING*

Capturing subsurface structures reveals geophysical facts related to climate change which are unseen by the human eye. Radar, due to its ability to penetrate non-conducting materials such as soil, sand and ice, is able to capture this information. An example for a relevant subsurface feature is the soil moisture, which is essential for growth of forests and crops and can be severely affected by long dry periods that could result from climate change. Another example is the internal structure of glaciers, which changes during the seasons from thawing and re-freezing and depends on the quantity of snowfall in winter. Both effects can be indicators of climate change when monitored over large time spans.

When measuring subsurface structures with radars on UAVs, the electromagnetic wave first travels through air and then penetrates the ground. Since the ground has different material parameters than air, wave propagation changes at the material interface. A typical characteristic of soil is high attenuation due to its naturally inhomogeneous structure and water/moisture content. Therefore, for subsurface imaging radars on UAVs, a typical choice of frequency is the upper MHz or lower GHz range [33]. Apart from attenuation, the ground material causes a decrease in propagation velocity and, as a consequence, refraction for non-normal incidence of the wave.

Various radar imaging techniques exist that are tailored particularly to subsurface imaging. The simplest one are B-scans, for which the UAV flies over the ground and measurements are taken with a down-looking antenna. Another option is SAR imaging for subsurface investigations. As an example, Fig. 6 shows a B-scan image and a SAR image of the Jungfraufirn glacier in Switzerland, revealing its subsurface structure.

Subsurface SAR image reconstruction algorithms include adaptation of the Backprojection algorithm as well as of the Omega-k algorithm. Whereas the Backprojection algorithm can be applied to any kind of material interface, Omega-k can be applied only to planar material interfaces. Algorithms for non-planar surfaces which are more efficient than the Backprojection algorithm include split-step-migration [77], phase-shift-plus-interpolation [78], or our recent works [36] and [79]. Compressed Sensing can be adapted to subsurface imaging as well, as shown for example in [80].

For subsurface SAR imaging with the Backprojection algorithm, the change in propagation velocity and the refraction have to be incorporated into the spatial matched filter for every pixel. When these effects are not considered, image distortions will occur which can amount to more than 90% compared to the true value [5]. To account for refraction, the refracted wave path has to be computed prior to imaging. Various techniques

exist for this purpose, such as ray tracing or a number of approximations [81], [82].

To properly determine the wave path, knowledge of the material boundary contour as well as of the permittivity is required. Whereas the boundary contour can be rather easily reconstructed by evaluating the first strong reflection in every image column (see, e.g., [83]), permittivity estimation for non-homogeneous media is not possible in a straightforward way. Thus, the material characteristics have to be modeled by investigating a sample from the ground, by burying a reference target at a reference depth or by reasonable empirical assumptions.

## IV. TOWARDS COOPERATIVE UAV SWARMS

In addition to using a single radar, UAVs provide the possibility of bi- and multistatic SAR by using a cooperative swarm. The transmitting and receiving nodes can be spatially distributed on separate platforms. The manifold opportunities and challenges of spaceborne and airborne bistatic and multistatic SAR have been discussed in a number of publications, e.g., [84], [85], [86], [87]. Due to the low cost and flexible operation of UAV-based radar systems, more nodes can be deployed in almost arbitrary configurations. This enables the simultaneous acquisition and evaluation of a larger variety and number of bistatic angles, offering new possible applications in climate research using UAVs as platform.

While, for these reasons, swarming is very promising, it also comes with a number of challenges:

- The relative positions of the two or more UAVs have to be known precisely.
- Accurate synchronization with respect to time, frequency, and phase between transmitter(s) and receiver(s) has to be achieved.
- Imaging algorithms have to be adapted to account for the distributed geometry of the transmit and receive antennas.
- Polarimetric imaging will depend heavily on the scene geometry.
- Calibration is another crucial issue, which has to be addressed.

In the following, we detail the aspects of bi-/ multistatic SAR as well as time synchronization and coherence.

### A. BI- AND MULTISTATIC SAR

Climate change effects, e.g., floods, droughts, and storms [9], can be directly measured with bi- or multistatic radar or SAR systems. A preferable approach in climate research is the measurement of essential long-term climate variables like biomass, soil moisture, or the ice extents in sea, land, and permafrost [3]. This allows a prediction of future climate change effects.

In recent years, many systems and concepts have been developed to estimate climate variables with bi- or multistatic radar systems. These systems are either space- or ground-based, which results in limitations in terms of the bistatic angle or the accessibility of the monitored area. Obtainable measurements include the extent of snow and ice [88], [89], [90], soil moisture [91], [92], biomass and deforestation data [11], [93], [94], freeze/thaw surface state retrieval [95], and the water body layer [8]. The limitations of these measurement techniques can be relaxed by using UAVs as sensor platforms. They offer a low-cost operation and multistatic systems are easy to scale [96]. Bi- and multistatic UAV-based systems have been presented for single-pass SAR tomography [16], interferometry [17], and for locating objects by evaluating forward scattered signals [97].

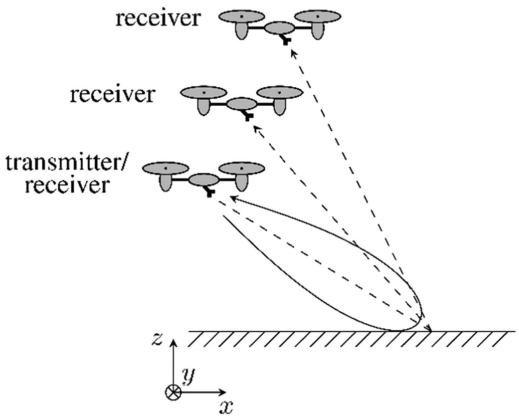


**FIGURE 7.** Schematic representation of a multistatic system with multiple UAVs for single-pass tomography. One sensor node is transmitting and receiving, the remaining nodes are receiving only.

The imaging techniques discussed in Section III can be extended to a cooperative swarm of UAVs. Bistatic or multistatic SAR enhances imaging by not only using the backscattered signal but also evaluating other scattering directions. This allows operation modes like single-pass interferometry and tomography, with the advantage of not having any temporal decorrelation within the jointly processed SAR images [3], [52].

Fig. 7 shows one possible implementation of a multistatic system for single-pass tomography, where one sensor is transmitting and receiving the backscattered signal like in a monostatic acquisition. The remaining sensor nodes form the multistatic system while only receiving backscattered signals with different observation angles. The additional bistatic information can be used to resolve further dimensions. Compared to space-based systems, large apertures with many platforms are feasible to ensure sufficient spatial sampling. Various effects normally coupled in monostatic acquisitions can be separated, resulting in the less ambiguous determination of climate-relevant parameters.

The large bistatic angle allows for new acquisition geometries compared to the conventional tomographic or interferometric techniques. Forward-scattered signals can be evaluated, providing complementary information to the backscattered signals. With UAVs operating in a swarm, multiple angles can be observed, opening up new possibilities in climate change research. This concept is illustrated in Fig. 8.

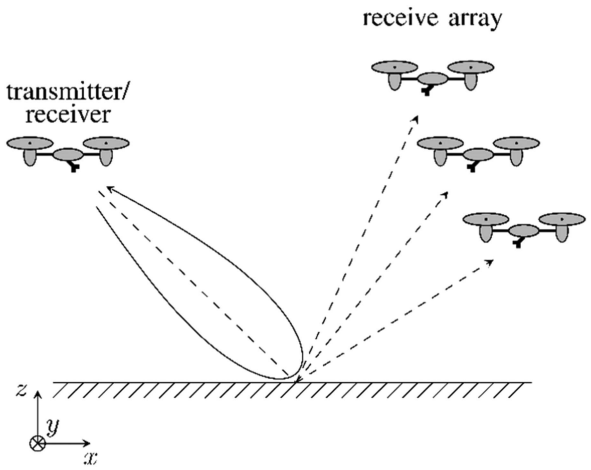


**FIGURE 8.** Schematic representation of a multistatic forward scattering system. One sensor node is transmitting and receiving the backscattered signal, the remaining nodes are receiving only and form an array that captures various scattering directions.

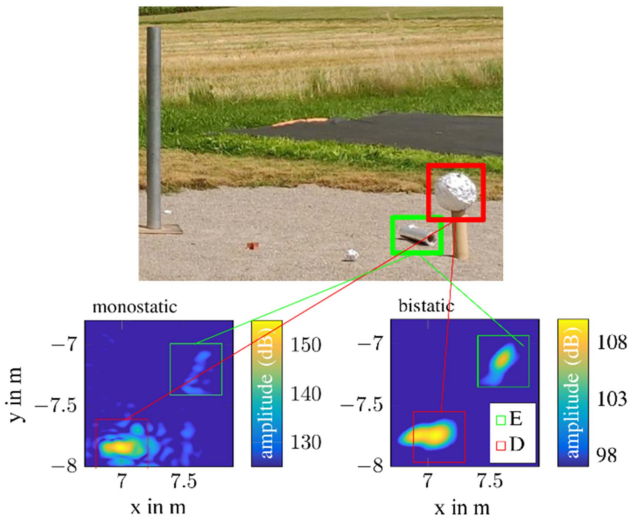


**FIGURE 9.** Measurement of various radar targets above ground with monostatic and bistatic SAR images. Results taken from [99].

The transmitting system is receiving the backscattered signal in monostatic operation, and the other systems are forming a receive array for covering a wide range of scattering directions. With this, more information about the scattering structure can be obtained, e.g., in natural environments with a strong angular dependency of scattering effects. While the ground range resolution is poor in forward scattering bistatic SAR, the depth dimension can be resolved [98]. This can be used to measure layered structures, e.g., ice layers inside a glacier or soil layers with varying permittivity.

Yet, various challenges have to be solved to successfully operate a bi- or multistatic UAV-based SAR system. These include processing the large bistatic angle, polarimetric evaluation, and the synchronization of the individual sensor nodes.

Conventional SAR processing cannot be directly applied to a bistatic geometry. For a small bistatic angle, there are approaches using a quasi-monostatic approximation. This is not feasible for UAV-based systems, where much larger bistatic angles are desired in order to capture a wide span of observation angles. Algorithms adapted to the geometry are therefore necessary. Time-domain backprojection has been proven feasible for SAR processing of geometries with a large bistatic angle [97], [99].

Polarimetric evaluation of bistatic SAR data is a field not yet widely addressed in current research. The lack of symmetry in the polarimetric backscattered matrix makes conventional polarimetric analyses difficult [100]. Despite this, it has been shown to be sensitive to parameters like soil moisture, wind speed, and freeze/thaw state, making it promising for climate change research [101]. Bistatic UAV-based systems could provide data not yet available using possibly new acquisition geometries.

Fig. 9 shows the monostatic and bistatic SAR images generated at the same time with a moving UAV-based radar and a stationary repeater [99]. The colorbars are referenced to the maximum value measured from the aluminum sphere. Although the dynamic range is higher in the monostatic image, the cylinder on the ground is only barely visible. In this measurement geometry, its bistatic RCS is much higher than its monostatic RCS. Therefore the measured amplitude of the cylinder target is higher in the bistatic image when compared to the aluminum sphere. This constitutes one example, where a bistatic measurement geometry can provide new information, leading to improved imaging capabilities.

### B. SYNCHRONIZATION AND COHERENCE

Synchronization is imperative in sensor fusion for distributed UAV multistatic radar systems, as each sensor has its own time base. An accurate time, frequency, and phase synchronization ensures precise localization, and enables coherent bistatic signal processing, which grants access to additional information about the observed scene, as discussed in the previous section. In specific applications such as climate monitoring, which necessitate joint radar processing across extensive surveillance areas, the precision of time, frequency, and phase synchronization is critical. This synchronization substantially enhances the resolution and reliability of measurements, facilitating the accurate alignment of data from multiple sensors. Such rigorous alignment is essential for conducting detailed analytical assessments necessary for detecting nuanced changes in climate patterns.

#### 1) PTP-BASED PRESYNCHRONIZATION

In our research [102], based on field-programmable gate arrays (FPGAs), real-time wireless digital communication systems have been implemented across radar sensors, allowing each radar node to establish a wireless connection to a centralized primary reference node. This configuration ensures optimal performance by maintaining consistent and precise pre-synchronization across the entire network. The radar nodes systematically update their timestamps through time

offset estimation, utilizing the Precision Time Protocol (PTP) at predetermined intervals. The radar nodes send synchronization requests to the primary reference node, achieving timing precision with a standard deviation of 10 nanoseconds per cycle. Furthermore, frequency offsets are ascertained through consecutive time offset estimations across the network. Subsequently, these offsets are meticulously compensated using digitally controlled crystal oscillators (DCTCXOs), achieving an exceptional level of precision of two parts per billion. This methodology underscores the integration of advanced pre-synchronization mechanisms to enhance the accuracy and reliability of netted radar systems.

Further signal processing with Kalman filtering additionally increases the pre-synchronization performance in terms of precision and real-time capability. In [103], the authors explore the development of positioning techniques that require the synchronization of multiple stations. The synchronization algorithm employs Kalman-filter-based clock synchronization in IEEE 1588 networks, as detailed in [104] and [105]. The system has been enhanced through the integration of the Kalman filter, significantly improving the real-time tracking of time offset and skew using the PTP protocol and timestamp exchange. By leveraging the prediction and correction capabilities of the Kalman filter, these advancements lead to enhanced overall performance in time-sensitive applications.

### 2) COHERENT BISTATIC PROCESSING

To achieve phase coherency between each pair of radar nodes in the multistatic network, in our recent work [106] we rely on a two-way radar-signalling scheme. For this, an over-the-air synchronization concept is applied to estimate the residual time, frequency, and phase errors and compensate them as described in. Then, we can take the compensated signals to derive the range and angle-of-arrival (AoA) information for every bistatic constellation, enabling a localization accuracy below 1 cm [107]. After these steps, a coherent image processing of the bistatic signals is possible (cf. [106]).

Besides the mentioned synchronization-based approach, several other approaches of coupling the nodes exist to accomplish coherency. Passive radar methods with a known transmitter, e.g., GNSS signals, represent a wide range of bistatic systems. The use of UAVs as receiver platform has been shown feasible for flood monitoring [108]. A similar approach is using a repeater, which re-transmits the received signal back to the transmitting system. This allows for coherent processing at only one node [97], [99].

Such a radar repeater network was used in [97] to localize objects in all three spatial dimensions by using both mono- and bistatic data. Fig. 10 shows a monostatic SAR image of a setup with various objects on ground focused at the height extracted from the bistatic data. Without the bistatic data, only two dimensions could be resolved. In a forward scattering geometry, the missing height information can be extracted from the bistatic data, as the energy is focused at the actual object height.

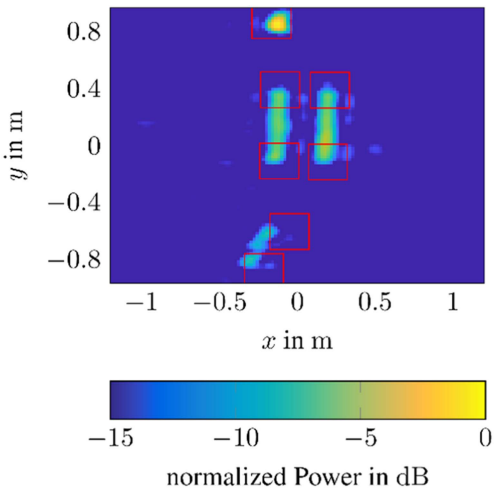


**FIGURE 10.** Measurement of various radar targets above ground. Monostatic SAR image focused at height extracted from bistatic data. Ground truth positions are marked by red boxes. Results taken from [97].

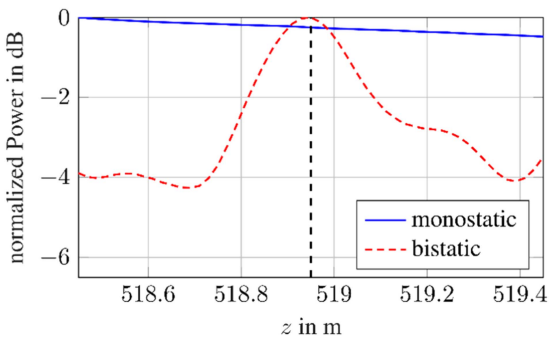


**FIGURE 11.** Height focusing curve extracted from mono- and bistatic SAR images by summing the squared pixel values for each height. Ground truth is marked by the vertical dashed line. Results taken from [97].

Fig. 11 shows the sum of the squared pixel values for the monostatic and bistatic SAR image focused at various heights $z$. Unlike the monostatic data, the bistatic data shows a peak at the correct height.

## V. CONCLUSION AND OUTLOOK

Radar remote sensing is well suited to monitor the multifaceted effects of climate change, such as changes in soil moisture and vegetation or the melting of glaciers and permafrost soils. Imaging radars can provide quantitative, graphical representations of these effects and report trends when monitoring over a longer period of time. While spaceborne radar imaging is well-established, UAV-based SAR imaging is becoming more and more attractive due to its benefits, which include flexibility, cost-efficiency, fast deployment, very high spatial resolution, and the opportunity for a quasi-continuous observation of local areas.

This article discussed various aspects associated with using UAV-based radar imaging for climate change monitoring. We showed that a number of approaches exist, both for system design and for imaging, depending on the respective application.

One future trend in this respect is the deployment of cooperative UAV swarms, which will enable even higher image quality and new multistatic SAR modes for tomographic and holographic 3D imaging. Thus, potentially, a higher information content will be possible, as discussed in this article. Another trend in evaluating the obtained images is the use of methods from artificial intelligence. This way, it will be possible to detect features in the data which are directly associated with climate change effects.

## REFERENCES


[1] A. Moreira, P. Prats-Iraola, M. Younis, G. Krieger, I. Hajnsek, and K. P. Papathanassiou, "A tutorial on synthetic aperture radar," *IEEE Geosci. Remote Sens. Mag.*, vol. 1, no. 1, pp. 6–43, Mar. 2013.

[2] A. Reigber et al., "Very-high-resolution airborne synthetic aperture radar imaging: Signal processing and applications," *Proc. IEEE*, vol. 101, no. 3, pp. 759–783, Mar. 2013.

[3] A. Moreira et al., "Tandem-L: A highly innovative bistatic SAR mission for global observation of dynamic processes on the earth's surface," *IEEE Geosci. Remote Sens. Mag.*, vol. 3, no. 2, pp. 8–23, Jun. 2015, doi: 10.1109/MGRS.2015.2437353.

[4] C. Elachi, K. E. Im, F. Li, and E. Rodriguez, "Global digital topography mapping with a synthetic aperture scanning radar altimeter," *Int. J. Remote Sens.*, vol. 11, no. 4, pp. 585–601, Apr. 1990.

[5] S. Tebaldini, T. Nagler, H. Rott, and A. Heilig, "Imaging the internal structure of an alpine glacier via L-band airborne SAR tomography," *IEEE Trans. Geosci. Remote Sens.*, vol. 54, no. 12, pp. 7197–7209, Dec. 2016, doi: 10.1109/TGRS.2016.2597361.

[6] J. J. Sharma, I. Hajnsek, K. P. Papathanassiou, and A. Moreira, "Estimation of glacier ice extinction using long-wavelength airborne Pol-InSAR," *IEEE Trans. Geosci. Remote Sens.*, vol. 51, no. 6, pp. 3715–3732, Jun. 2013, doi: 10.1109/TGRS.2012.2220855.

[7] A. Benedikter, M. Rodriguez-Cassola, F. Betancourt-Payan, G. Krieger, and A. Moreira, "Autofocus-based estimation of penetration depth and permittivity of ice volumes and snow using single SAR images," *IEEE Trans. Geosci. Remote Sens.*, vol. 60, 2022, Art. no. 4303315.

[8] M. Zink et al., "TanDEM-X: 10 years of formation flying bistatic SAR interferometry," *IEEE J. Sel. Topics Appl. Earth Observ. Remote Sens.*, vol. 14, pp. 3546–3565, 2021, doi: 10.1109/JSTARS.2021.3062286.

[9] T. Jagdhuber, I. Hajnsek, H. Schoen, and K. P. Papathanassiou, "Pol-SAR time series for soil moisture estimation under vegetation," in *Proc. IEEE 7th Eur. Conf. Synthetic Aperture Radar*, Friedrichshafen, Germany, 2008, pp. 1–4.

[10] H. Joerg, M. Pardini, A. Alonso-Gonzalez, K. P. Papathanassiou, and I. Hajnsek, "Investigating soil moisture dependency of the ground polarimetry under agricultural vegetation estimated by SAR tomography," in *Proc. IEEE 12th Eur. Conf. Synthetic Aperture Radar*, Aachen, Germany, 2018, pp. 1–5.

[11] M. Lavalle et al., "Distributed aperture radar tomographic sensors (DARTS) to map surface topography and vegetation structure," in *Proc. IEEE Int. Geosci. Remote Sens. Symp.*, Brussels, Belgium, 2021, pp. 1090–1093, doi: 10.1109/IGARSS47720.2021.9553170.

[12] S. Lee, F. Kugler, I. Hajnsek, and K. Papathanassiou, "The potential and challenges of polarimetric SAR interferometry techniques for forest parameter estimation at P-band," in *Proc. IEEE 8th Eur. Conf. Synthetic Aperture Radar*, Aachen, Germany, 2010, pp. 1–3.

[13] R. Burr, M. Schartel, P. Schmidt, W. Mayer, T. Walter, and C. Waldschmidt, "Design and implementation of a FMCW GPR for UAV-based mine detection," in *Proc. IEEE MTT-S Int. Conf. Microw. Intell. Mobility*, Munich, Germany, 2018, pp. 1–4, doi: 10.1109/ICMIM.2018.8443526.

[14] Y. A. Lopez, M. Garcia-Fernandez, G. Alvarez-Narciandi, and F. L.-H. Andres, "Unmanned aerial vehicle-based ground-penetrating radar systems: A review," *IEEE Geosci. Remote Sens. Mag.*, vol. 10, no. 2, pp. 66–86, Jun. 2022.

[15] A. Grathwohl et al., "Taking a look beneath the surface: Multicopter UAV-based ground-penetrating imaging radars," *IEEE Microw. Mag.*, vol. 23, no. 10, pp. 32–46, Oct. 2022.

[16] Y. Wang et al., "First demonstration of single-pass distributed SAR tomographic imaging with a P-band UAV SAR prototype," *IEEE Trans. Geosci. Remote Sens.*, vol. 60, 2022, Art. no. 5238618.

[17] S.-Y. Jeon et al., "Experimental demonstration of bistatic UAV-borne SAR and InSAR," in *Proc. 15th Eur. Conf. Synthetic Aperture Radar*, 2024, pp. 1150–1155.

[18] J. Svedin, A. Bernland, and A. Gustafsson, "Small UAV-based high resolution SAR using low-cost radar, GNSS/RTK and IMU sensors," in *Proc. IEEE 17th Eur. Radar Conf.*, 2021, pp. 186–189.

[19] C. Noviello, G. Esposito, G. Fasano, A. Renga, F. Soldovieri, and I. Catapano, "Small-UAV radar imaging system performance with GPS and CDGPS based motion compensation," *Remote Sens.*, vol. 12, Oct. 2020, Art. no. 3463.

[20] M. Otten, N. Maas, R. Bolt, M. Caro-Cuenca, and K. Henk Medenblik, "Circular micro-SAR for mini-UAV," in *Proc. IEEE 15th Eur. Radar Conf.*, 2018, pp. 321–324.

[21] M. Lort, A. Aguasca, C. Lopez-Martinez, and T. M. Marin, "Initial evaluation of SAR capabilities in UAV multicopter platforms," *IEEE J. Sel. Topics Appl. Earth Observ. Remote Sens.*, vol. 11, no. 1, pp. 127–140, Jan. 2018.

[22] F. Brigui, S. Angelliaume, N. Castet, X. Dupuis, and P. Martineau, "SAR-light - first SAR images from the new Onera SAR sensor on UAV platform," in *Proc. IEEE Int. Geosci. Remote Sens. Symp.*, 2022, pp. 7721–7724.

[23] M. Wielgo, D. Gromek, P. Samczynski, K. Stasiak, and M. Gawel, "Low-cost high-resolution SAR imaging on drone with mechanical antenna stabilization," in *Proc. IEEE 23rd Int. Radar Symp.*, 2022, pp. 83–86.

[24] M. R. P. Cerquera, J. D. C. Montaño, and I. Mondragón, "UAV for landmine detection using SDR-based GPR technology," in *Robots Operating in Hazardous Environments*. Rijeka, Croatia: InTech, 2017, pp. 25–58.

[25] D. Šipoš and D. Gleich, "A lightweight and low-power UAV-borne ground penetrating radar design for landmine detection," *Sensors*, vol. 20, Apr. 2020, Art. no. 2234.

[26] M. García-Fernández, G. Álvarez-Narciandi, F. L. Heras, and Y. Álvarez-López, "Comparison of scanning strategies in UAV-mounted multichannel GPR-SAR systems using antenna arrays," *IEEE J. Sel. Topics Appl. Earth Observ. Remote Sens.*, vol. 17, pp. 3571–3586, 2024.

[27] M. Schartel, R. Burr, R. Bähnemann, W. Mayer, and C. Waldschmidt, "An experimental study on airborne landmine detection using a circular synthetic aperture radar," 2020, *arXiv:2005.02600*.

[28] A. Grathwohl, P. Hinz, R. Burr, M. Steiner, and C. Waldschmidt, "Experimental study on the detection of avalanche victims using an airborne ground penetrating synthetic aperture radar," in *Proc. IEEE Radar Conf.*, 2021, pp. 1–6.

[29] G. Oré et al., "Drone borne SAR tomography as a powerful subsurface survey tool," in *Proc. IEEE 8th Asia-Pacific Conf. Synthetic Aperture Radar*, 2023, pp. 1–4.

[30] A. E.-C. Tan, J. McCulloch, W. Rack, I. Platt, and I. Woodhead, "Radar measurements of snow depth over sea ice on an unmanned aerial vehicle," *IEEE Trans. Geosci. Remote Sens.*, vol. 59, no. 3, pp. 1868–1875, Mar. 2021.

[31] R. O. R. Jenssen, M. Eckerstorfer, S. K. Jacobsen, and R. Storvold, "Drone-mounted UWB radar system for measuring snowpack properties: Technical implementation, specifications and initial results," in *Proc. Int. Snow Sci. Workshop*, Innsbruck, Austria, 2018, pp. 673–676.

[32] S. Prager, G. Sexstone, D. McGrath, J. Fulton, and M. Moghaddam, "Snow depth retrieval with an autonomous UAV-mounted software-defined radar," *IEEE Trans. Geosci. Remote Sens.*, vol. 60, 2022, Art. no. 5104816.

[33] M. Stelzig et al., "A drone-based 0.7-4.7 GHz FMCW radar system for high-resolution exploration of subsurface glacier structures," in *Proc. IEEE Int. Radar Conf.*, 2023, pp. 1–6.

[34] K. Wu and S. Lambot, "Analysis of low-frequency drone-borne GPR for root-zone soil electrical conductivity characterization," *IEEE Trans. Geosci. Remote Sens.*, vol. 60, 2022, Art. no. 2006213.

[35] H. Rudolf, D. Tarchi, and A. J. Sieber, "Combination of linear and circular SAR for 3-D features," in *Proc. IEEE Int. Geosci. Remote Sens. Symp. Remote Sens. - Sci. Vis. Sustain. Develop.*, 1997, vol. 4, pp. 1551–1553.

[36] A. Grathwohl, B. Arendt, T. Grebner, and C. Waldschmidt, "Detection of objects below uneven surfaces with a UAV-based GPSAR," *IEEE Trans. Geosci. Remote Sens.*, vol. 61, 2023, Art. no. 5207913.

[37] P. Stockel, P. Wallrath, R. Herschel, and N. Pohl, "Motion compensation in six degrees of freedom for a MIMO radar mounted on a hovering UAV," *IEEE Trans. Aerosp. Electron. Syst.*, vol. 59, no. 5, pp. 5791–5801, Oct. 2023.

[38] K. T. J. Klein, F. Uysal, M. C. Cuenca, M. P. G. Otten, and J. J. M. de Wit, "Motion estimation and improved SAR imaging for agile platforms using omnidirectional radar and INS sensor fusion," *IEEE Trans. Aerosp. Electron. Syst.*, vol. 59, no. 1, pp. 153–171, Feb. 2023.

[39] A. Bekar, M. Antoniou, and C. J. Baker, "Low-cost, high-resolution, drone-borne SAR imaging," *IEEE Trans. Geosci. Remote Sens.*, vol. 60, 2022, Art. no. 5208811.

[40] J. Colorado, C. Devia, M. Perez, I. Mondragon, D. Mendez, and C. C. Parra, "Low-altitude autonomous drone navigation for landmine detection purposes," in *Proc. IEEE Int. Conf. Unmanned Aircr. Syst.*, 2017, pp. 540–546.

[41] R. Bähnemann et al., "Under the sand: Navigation and localization of a micro aerial vehicle for landmine detection with ground-penetrating synthetic aperture radar," *Field Robot.*, vol. 2, pp. 1028–1067, 2022, doi: 10.55417/fr.2022034.

[42] F. Xu et al., "Heuristic path planning method for multistatic UAV-borne SAR imaging system," *IEEE J. Sel. Topics Appl. Earth Observ. Remote Sens.*, vol. 14, pp. 8522–8536, 2021, doi: 10.1109/JSTARS.2021.3106449.

[43] Z. Guan, Z. Sun, J. Wu, and J. Yang, "Resource allocation and optimization of multi-UAV SAR system," in *Proc. IEEE RadarConf23*, San Antonio, TX, USA, May 2023, pp. 1–5, doi: 10.1109/RadarConf2351548.2023.10149786.

[44] Z. Sun, H. Sun, H. An, Z. Li, J. Wu, and J. Yang, "Trajectory optimization for maneuvering platform bistatic SAR with geosynchronous illuminator," *IEEE Trans. Geosci. Remote Sens.*, vol. 62, 2024, Art. no. 5203715, doi: 10.1109/TGRS.2024.3358303.

[45] S. Hu, X. Yuan, W. Ni, and X. Wang, "Trajectory planning of cellular-connected UAV for communication-assisted radar sensing," *IEEE Trans. Commun.*, vol. 70, no. 9, pp. 6385–6396, Sep. 2022, doi: 10.1109/TCOMM.2022.3195868.

[46] M.-A. Lahmeri, W. Ghanem, C. Knill, and R. Schober, "Trajectory and resource optimization for UAV synthetic aperture radar," in *Proc. IEEE Globecom Workshops*, Dec. 2022, pp. 897–903, doi: 10.1109/GCWkshps56602.2022.10008658.

[47] M.-A. Lahmeri, W. R. Ghanem, C. Bonfert, and R. Schober, "Robust trajectory and resource optimization for communication-assisted UAV SAR sensing," *IEEE Open J. Commun. Soc.*, vol. 5, pp. 3212–3228, 2024, doi: 10.1109/OJCOMS.2024.3396922.

[48] M.-A. Lahmeri, V. Mustieles-Pérez, M. Vossiek, G. Krieger, and R. Schober, "UAV formation optimization for communication-assisted InSAR sensing," in *Proc. IEEE Int. Conf. Commun.*, Denver, CO, USA, 2024, pp. 3913–3918.

[49] R. H. Stolt, "Migration by Fourier transform," *Geophysics*, vol. 43, no. 1, pp. 23–48, 1978.

[50] R. Bamler and P. Hartl, "Synthetic aperture radar interferometry," *Inverse Problems*, vol. 14, Aug. 1998, Art. no. 4.

[51] G. Krieger, I. Hajnsek, K. P. Papathanassiou, M. Younis, and A. Moreira, "Interferometric synthetic aperture radar (SAR) missions employing formation flying," *Proc. IEEE*, vol. 98, no. 5, pp. 816–843, May 2010, doi: 10.1109/JPROC.2009.2038948.

[52] G. Krieger et al., "TanDEM-X: A satellite formation for high-resolution SAR interferometry," *IEEE Trans. Geosci. Remote Sens.*, vol. 45, no. 11, pp. 3317–3341, Nov. 2007.

[53] V. Mustieles-Perez, S. Kim, C. Bonfert, G. Krieger, and M. Villano, "Towards UAV-based ultra-wideband multi-baseline SAR interferometry," in *Proc. IEEE 20th Eur. Radar Conf.*, Berlin, Germany, 2023, pp. 233–236.

[54] M. Pinheiro, A. Reigber, R. Scheiber, P. Prats-Iraola, and A. Moreira, "Generation of highly accurate DEMs over flat areas by means of dual-frequency and dual-baseline airborne SAR interferometry," *IEEE Trans. Geosci. Remote Sens.*, vol. 56, no. 8, pp. 4361–4390, Aug. 2018.

[55] M. Pinheiro, A. Reigber, and A. Moreira, "Large-baseline InSAR for precise topographic mapping: A framework for TanDEM-X large-baseline data," *Adv. Radio Sci.*, vol. 15, pp. 231–241, 2017.

[56] V. Mustieles-Perez et al., "Experimental demonstration of UAV-based ultra-wideband multi-baseline SAR bnterferometry," in *Proc. Eur. Conf. Synthetic Aperture Radar*, 2024, pp. 1156–1161.

[57] S. Kim, G. Krieger, and M. Villano, "Volume structure retrieval using drone-based SAR interferometry with wide fractional bandwidth," *Remote Sens.*, vol. 16, 2024, Art. no. 1352, doi: 10.3390/rs16081352.

[58] S. Kim et al., "Demonstration of frequency-dependent penetration depth estimation using SAR interferometry with wide fractional bandwidth," in *Proc. IEEE Int. Geosci. Remote Sens. Symp.*, Sensing Symposium, Athens, Greece, 2024, pp. 10889–10893, doi: 10.1109/IGARSS53475.2024.10642476.

[59] O. Frey and E. Meier, "3-D time-domain SAR imaging of a forest using airborne multibaseline data at L- and P-bands," *IEEE Trans. Geosci. Remote Sens.*, vol. 49, no. 10, pp. 3660–3664, Oct. 2011.

[60] D. Ho Tong Minh, S. Tebaldini, F. Rocca, T. Le Toan, L. Villard, and P. C. Dubois-Fernandez, "Capabilities of BIOMASS tomography for investigating tropical forests," *IEEE Trans. Geosci. Remote Sens.*, vol. 53, no. 2, pp. 965–975, Feb. 2015.

[61] A. Reigber and A. Moreira, "First demonstration of airborne SAR tomography using multibaseline L-band data," *IEEE Trans. Geosci. Remote Sens.*, vol. 38, no. 5, pp. 2142–2152, Sep. 2000.

[62] M. Schartel, K. Prakasan, P. Hugler, R. Burr, W. Mayer, and C. Waldschmidt, "A multicopter-based focusing method for ground penetrating synthetic aperture radars," in *Proc. IEEE Int. Geosci. Remote Sens. Symp.*, Valencia, Spain, 2018, pp. 5420–5423.

[63] X. X. Zhu and R. Bamler, "Superresolving SAR tomography for multidimensional imaging of urban areas: Compressive sensing-based TomoSAR inversion," *IEEE Signal Process. Mag.*, vol. 31, no. 4, pp. 51–58, Jul. 2014.

[64] D. L. Donoho, "Compressed sensing," *IEEE Trans. Inf. Theory*, vol. 52, no. 4, pp. 1289–11306, Apr. 2006.

[65] L. C. Potter, E. Ertin, J. T. Parker, and M. Cetin, "Sparsity and compressed sensing in radar imaging," *Proc. IEEE*, vol. 98, no. 6, pp. 1006–1020, Jun. 2010.

[66] L. Zhao, L. Wang, L. Yang, A. M. Zoubir, and G. Bi, "The race to improve radar imagery: An overview of recent progress in statistical sparsity-based techniques," *IEEE Signal Process. Mag.*, vol. 33, no. 6, pp. 85–102, Nov. 2016.

[67] M. Çetin et al., "Sparsity-driven synthetic aperture radar imaging: Reconstruction, autofocusing, moving targets, and compressed sensing," *IEEE Signal Process. Mag.*, vol. 31, no. 4, pp. 27–40, Jul. 2014.

[68] Z. Wang, Z. Ding, T. Sun, J. Zhao, Y. Wang, and T. Zeng, "UAV-based P-band SAR tomography with long baseline: A multimaster approach," *IEEE Trans. Geosci. Remote Sens.*, vol. 61, 2023, Art. no. 5207221.

[69] S. Gao et al., "A robust super-resolution gridless imaging framework for UAV-borne SAR tomography," *IEEE Trans. Geosci. Remote Sens.*, vol. 62, 2024, Art. no. 5210917.

[70] C. Bonfert, E. Ruopp, and C. Waldschmidt, "Improving SAR imaging by superpixel-based compressed sensing and backprojection processing," *IEEE Trans. Geosci. Remote Sens.*, vol. 62, 2024, Art. no. 5209212.

[71] E. Aguilera, M. Nannini, and A. Reigber, "A data-adaptive compressed sensing approach to polarimetric SAR tomography of forested areas," *IEEE Geosci. Remote Sens. Lett.*, vol. 10, no. 3, pp. 543–547, May 2013.

[72] D. L. Donoho, A. Maleki, and A. Montanari, "Message passing algorithms for compressed sensing," *Proc. Nat. Acad. Sci.*, vol. 106, pp. 18914–18919, 2009.

[73] E. Sterk, C. Sippel, and R. F. H. Fischer, "Comparison of damping approaches for AMP," in *Proc. IEEE 26th Int. ITG Workshop Smart Antennas 13th Conf. Syst., Commun., Coding*, 2023, pp. 1–6.

[74] R. F. H. Fischer and C. Sippel, "Unbiasing in iterative reconstruction algorithms for discrete compressed sensing," in *Compressed Sensing in Information Processing*, G. Kutyniok, H. Rauhut, and R. J. Kunsch, Eds. Cambridge, MA, USA: Birkhaüser, Oct. 2022, pp. 181–212.

[75] A. Maleki, L. Anitori, Z. Yang, and R. G. Baraniuk, "Asymptotic analysis of complex LASSO via complex approximate message passing (CAMP)," *IEEE Trans. Inf. Theory*, vol. 59, no. 7, pp. 4290–4308, Jul. 2013.

[76] L. Anitori, A. Maleki, M. Otten, R. G. Baraniuk, and P. Hoogeboom, "Design and analysis of compressed sensing radar detectors," *IEEE Trans. Signal Process.*, vol. 61, no. 4, pp. 813–827, Feb. 2013.

[77] P. L. Stoffa, J. T. Fokkemat, R. M. de Luna Freire, and W. P. Kessinger, "Split-step fourier migration," *Geophysics*, vol. 55, no. 4, pp. 410–421, Apr. 1990, doi: 10.1190/1.1442850.

[78] J. Gazdag and P. Sguazzero, "Migration of seismic data by phase shift plus interpolation," *Geophysics*, vol. 49, no. 2, pp. 124–131, 1984, doi: 10.1190/1.1441643.

[79] I. Ullmann and M. Vossiek, "A novel, efficient algorithm for subsurface radar imaging below a non-planar surface," *Sensors*, vol. 23, no. 22, Nov. 2023, Art. no. 9021, doi: 10.3390/s23229021.

[80] Q. Yang, A. Zhang, Y. Jiang, and Y. Wang, "GPR imaging algorithm of targets located in layered mediums based on CS," in *Proc. IEEE 14th Int. Conf. Ground Penetrating Radar*, 2012, pp. 371–375.

[81] A. Heinzel et al., "Focusing method for ground penetrating MIMO SAR imaging within half-spaces of different permittivity," in *Proc. IEEE Eur. Conf. Synthetic Aperture Radar*, 2016, pp. 842–846.

[82] M. Stelzig et al., "A UAV-based radar sounder SAR Sytem for the imaging of internal snow and firn stratifications," in *Proc. 15th Eur. Conf. Synthetic Aperture Radar*, 2024, pp. 1135–1140.

[83] P. D. Walker and M. R. Bell, "Non-iterative GPR imaging through a non-planar air-ground interface," in *Proc. IEEE Int. Geosci. Remote Sens. Symp.*, 2001, vol. 3, pp. 1527–1529.

[84] A. Moccia, N. Chiacchio, and A. Capone, "Spaceborne bistatic synthetic aperture radar for remote sensing applications," *Int. J. Remote Sens.*, vol. 21, no. 18, pp. 3395–3414, 2000.

[85] D. Massonnet, "Capabilities and limitations of the interferometric cartwheel," *IEEE Trans. Remote Sens.*, vol. 39, no. 3, pp. 506–520, Mar. 2001.

[86] G. Krieger and A. Moreira, "Spaceborne bi-and multistatic SAR: Potential and challenges," *IEE Proc.-Radar, Sonar Navigation*, vol. 153, no. 3, pp. 184–198, 2006.

[87] M. Cherniakov, Ed., *Bistatic Radar: Emerging Technology*. Hoboken, NJ, USA: Wiley, 2008.

[88] G. Luzi et al., "Monitoring of an alpine glacier by means of ground-based SAR interferometry," *IEEE Geosci. Remote Sens. Lett.*, vol. 4, no. 3, pp. 495–499, Jul. 2007.

[89] J. H. H. Eriksrod, J. F. Burkhart, T. S. Lande, and S.-E. Hamran, "Bistatic SAR radar for long-term snow pack monitoring," *IEEE Trans. Geosci. Remote Sens.*, vol. 58, no. 1, pp. 218–226, Jan. 2020.

[90] M. Stefko, P. Bernhard, O. Frey, and I. Hajnsek, "Polarimetric analysis of biseasonal monostatic and bistatic radar observations of a glacier accumulation zone at Ku-band," *IEEE J. Sel. Topics Appl. Earth Observ. Remote Sens.*, vol. 17, pp. 9706–9727, 2024.

[91] V. Zavorotny et al., "Seasonal polarimetric measurements of soil moisture using tower-based GPS bistatic radar," in *Proc. IEEE Int. Geosci. Remote Sens. Symp.*, 2003, vol. 2, pp. 781–783.

[92] N. Pierdicca et al., "The potential of spaceborne GNSS reflectometry for soil moisture, biomass, and freeze–thaw monitoring: Summary of a European space agency-funded study," *IEEE Geosci. Remote Sens. Mag.*, vol. 10, no. 2, pp. 8–38, Jun. 2022.

[93] F. Kugler, D. Schulze, I. Hajnsek, H. Pretzsch, and K. P. Papathanassiou, "TanDEM-X Pol-InSAR performance for forest height estimation," *IEEE Trans. Geosci. Remote Sens.*, vol. 52, no. 10, pp. 6404–6422, Oct. 2014.

[94] A. Torano Caicoya, F. Kugler, I. Hajnsek, and K. P. Papathanassiou, "Large-scale biomass classification in boreal forests with TanDEM-X data," *IEEE Trans. Geosci. Remote Sens.*, vol. 54, no. 10, pp. 5935–5951, Oct. 2016.

[95] H. Carreno-Luengo and C. S. Ruf, "Mapping freezing and thawing surface state periods with the CYGNSS based F/T seasonal threshold algorithm," *IEEE J. Sel. Topics Appl. Earth Observ. Remote Sens.*, vol. 15, pp. 9943–9952, 2022.

[96] M. Villano et al., "Potential of multi-static SAR systems for earth monitoring and their demonstration using swarms of drones," in *2023 IEEE Int. Geosci. Remote Sens. Symp.*, 2023, pp. 4586–4589.

[97] J. Kanz, C. Bonfert, R. Riekenbrauck, and C. Waldschmidt, "Bistatic UAV-based repeater SAR for 3D object localization," in *Proc. Eur. Conf. Synthetic Aperture Radar*, 2024, pp. 1144–1149.

[98] T. Zeng, M. Cherniakov, and T. Long, "Generalized approach to resolution analysis in vol," *IEEE Trans. Aerosp. Electron. Syst.*, vol. 41, no. 2, pp. 461–474, Apr. 2005.

[99] A. Grathwohl, B. Meinecke, M. Widmann, J. Kanz, and C. Waldschmidt, "UAV-based bistatic SAR-imaging using a stationary repeater," *IEEE J. Microwaves*, vol. 3, no. 2, pp. 625–634, Apr. 2023, doi: 10.1109/JMW.2023.3253667.

[100] Y. Wang, T. L. Ainsworth, and J.-S. Lee, "On the geometrical dependency of the polarimetric bistatic SAR observation," in *Proc. IEEE Int. Geosci. Remote Sens. Symp.*, 2019, pp. 4935–4938.

[101] J. F. Munoz-Martin, N. Rodriguez-Alvarez, X. Bosch-Lluis, and K. Oudrhiri, "Stokes parameters retrieval and calibration of hybrid compact polarimetric GNSS-R signals," *IEEE Trans. Geosci. Remote Sens.*, vol. 60, 2022, Art. no. 5113911.

[102] R. Ghasemi, T. Koegel, P. Fenske, R. Schober, and M. Vossiek, "Time and frequency synchronization for real-time wireless digital communication systems," in *Proc. IEEE 15th German Microw. Conf.*, Duisburg, Germany, 2024, pp. 13–16, doi: 10.23919/GeMiC59120.2024.10485238.

[103] J. Cano, S. Chidami, and J. L. Ny, "A kalman filter-based algorithm for simultaneous time synchronization and localization in UWB networks," in *Proc. IEEE Int. Conf. Robot. Automat.*, Montreal, QC, Canada, 2019, pp. 1431–1437, doi: 10.1109/ICRA.2019.8794180.

[104] G. Giorgi and C. Narduzzi, "Performance analysis of kalman-filter-based clock synchronization in IEEE 1588 networks," *IEEE Trans. Instrum. Meas.*, vol. 60, no. 8, pp. 2902–2909, Aug. 2011, doi: 10.1109/TIM.2011.2113120.

[105] M. Hamer and R. D'Andrea, "Self-calibrating ultra-wideband network supporting multi-robot localization," *IEEE Access*, vol. 6, pp. 22292–22304, 2018, doi: 10.1109/ACCESS.2018.2829020.

[106] P. Fenske, T. Koegel, R. Ghasemi, and M. Vossiek, "Constellation estimation, coherent signal processing, and multiperspective imaging in an uncoupled bistatic cooperative radar network," *IEEE J. Microwaves*, vol. 4, no. 3, pp. 486–500, Jul. 2024, doi: 10.1109/JMW.2024.3393120.

[107] P. Fenske, S. Brueckner, T. Koegel, and M. Vossiek, "A novel concept for vehicle 2D pose estimation using automotive SIMO FMCW radar sensors in a bistatic vehicle-to-infrastructure network," in *Proc. IEEE Radar Conf.*, 2024, pp. 1–6.

[108] R. Imam, M. Pini, G. Marucco, F. Dominici, and F. Dovis, "Data from GNSS-based passive radar to support flood monitoring operations," in *Proc. IEEE Int. Conf. Localization GNSS*, 2019, pp. 1–7.